

Biparametric calibrations of stellar mass, radius and surface gravity using uvby- H_{β} photometry

I. Ribas¹, C. Jordi¹, J. Torra¹, and A. Giménez²

¹ Departament d'Astronomia i Meteorologia, Universitat de Barcelona, Avda. Diagonal 647, E-08028 Barcelona, Spain

² INTA-LAEFF, Apartado 50727, E-28080 Madrid, Spain

Received 14 April 1997 / Accepted 18 June 1997

Abstract. The aim of this study is to construct biparametric calibrations to estimate masses, radii and surface gravities for main-sequence stars using a photometric index related to effective temperature and another related to evolution.

For this purpose, we used a sample of detached double-lined eclipsing binaries with accurate ($\approx 1\text{-}2\%$) determinations of mass and radius and with available Strömgen–Crawford photometry for the individual components of the binary system.

The accuracies obtained, for the predicted dimensions when applied to single stars, are about 5–8% in mass, 10–15% in radius and 0.08–0.10 dex in surface gravity for stars in the main sequence with T_{eff} in the range between 7000 K and 20000 K. Precisions are thus considerably better than those obtained through single-parameter calibrations (using spectral type, T_{eff} or one colour index), and comparable to those derived through model atmospheres and stellar evolutionary models, of much higher complexity.

Key words: stars: fundamental parameters – stars: binaries: eclipsing – stars: early-type – stars: late-type – stars: general

1. Introduction

The estimation of stellar masses, radii, luminosities and chemical compositions is of fundamental astrophysical interest, since these parameters describe the properties and evolution of stars and hence the principal components of stellar clusters and galaxies.

The mass of a star can be determined directly only through its gravitational interaction with surrounding bodies, such as planets or other observable stars in multiple stellar systems. The stellar radius can be determined for eclipsing binaries and using interferometric techniques or occultations for single nearby

stars. Nevertheless, light and radial velocity curves of double-lined eclipsing binaries provide accurate and simultaneous determinations of masses, radii and luminosity ratios. The latter, for each photometric band, allows us to derive the individual photometric indices of each of the components of the system.

For most single stars, the mass and the radius can be inferred from observable (photometric or spectroscopic) parameters, calibrated by means of well-observed binary stars. Detached double-lined eclipsing binaries constitute the necessary database for the construction of such calibrations since no mass transfer has occurred between the components and they can be assumed to have evolved as single stars.

Binaries of this kind have also been used to normalize synthetic spectra given by stellar model atmospheres, and to place some constraints on the construction of stellar evolutionary models. The interpolation in these models, using photometric indices as input values, allows us then to estimate the mass, radius and surface gravity of single stars. A detailed description of this procedure can be found in Figueras et al. (1991), Jordi et al. (1997, Paper I) and Asiain et al. (1997). However, the application of this method implies the use of non-trivial algorithms to interpolate both in the photometric grids (which relate the atmospheric parameters with the photometric indices) and in the evolutionary models. For this reason, the estimation of masses, radii and surface gravities for single stars is still frequently performed by means of uniparametric calibrations, using T_{eff} , a colour index, or the spectral type as the free parameter, and without taking into account evolutionary effects within the main sequence. Many such single-parameter calibrations can be found in the literature (Allen 1973, Habets & Heintze 1981, Straižys & Kuriliene 1981, Schmidt-Kaler 1982, Van Hamme & Wilson 1986, among others) mainly using MK spectral types. Due to the width of the main sequence, these calibrations carry an uncertainty of about 15% in mass and 50% in radius (Nordström 1989, Andersen 1991).

To improve the situation, the natural step forward is the construction of two-parameter calibrations to compute masses, radii and surface gravities. A first attempt in this direction was made by Balona (1984), who used the evolutionary models of

Becker (1981) and Maeder (1981) and the Strömgen-Crawford c_o and β indices for early type stars. The precision achieved was similar to that of single-parameter calibrations, but was later improved by a factor of two by Balona (1994) when using a sample of better quality and different evolutionary models (Claret & Giménez 1992, Schaller et al. 1992, hereafter SSMM).

The use of accurate eclipsing binary data for the construction of biparametric mass, radius and surface gravity calibrations in terms of Strömgen-Crawford photometric indices is the aim of the present work.

2. The sample

The database is composed of detached double-lined eclipsing binary systems having M and R determinations with an accuracy of 1-2% as well as *uvby-H_β* photometry for each component of the system. The 53 stars in the sample, belonging to 30 binary systems, are listed in Table 5 of Paper I, together with a description of the spectral type distribution and the mass and evolutionary ranges covered. The empirical determinations of M , R and $\log g$ were taken from Andersen (1991), Nordström & Johansen (1994a, 1994b) and Clausen (1996).

Considering Strömgen's (1966) classification of stars in different regions of the HR diagram, the sample was divided into 22 stars in the early region, 6 stars in the intermediate region and 25 stars in the late region.

3. Calibrations

Taking into account the qualitative similarities of the evolutionary changes in radius and luminosity for a given mass, in terms of the effective temperature, when compared to absolute magnitude, Andersen (1991) suggested the construction of mass, radius and surface gravity calibrations in an equivalent way to the absolute magnitude calibrations of Crawford (1975, 1978, 1979), i.e. using a relation for the ZAMS and taking into account the evolutionary stage of each star.

Thus, the general form of the proposed equations becomes:

$$\log q = \log q_{\text{ZAMS}}(c_T) + f_q \delta c_g(c_T) \quad (1)$$

where q denotes in each case M , R and g in units of M_\odot , R_\odot and cgs , respectively, c_T and c_g are intrinsic photometric indices related to effective temperature and surface gravity, $\log q_{\text{ZAMS}}(c_T)$ stands for the relation of the ZAMS stars as a function of c_T , and $f_q \delta c_g$ is the term that accounts for the evolution of the star. Depending on the photometric region, c_T and c_g have different correspondences with Strömgen-Crawford indices. Thus, c_o and β , a_o and r , β and c_o are the c_T and c_g indices for the early, intermediate and late regions, respectively.

Andersen (1991), considering that the coefficient of the evolutionary term in Crawford's (1975, 1978, 1979) absolute magnitude calibrations was always close to -10 , assumed that $\Delta\beta$ and δc_o , defined as $\Delta\beta = \beta_{\text{ZAMS}}(c_o) - \beta$ and $\delta c_o = c_o - c_{o\text{ZAMS}}(\beta)$, both have the same evolutionary scale factor. Thus, f_M , f_R and f_g ought to be independent of the photometric

region. Due to the lack of complete *uvby-H_β* individual photometry for many of the binaries in his data sample and the small number of systems near to the ZAMS, he used stars, belonging to different binaries, with almost identical effective temperatures but different degrees of evolution to obtain differences in both the physical quantities and the absolute magnitude. In this way, assuming -10 for all regions when relating ΔM_V and δc_g , he estimated the evolutionary factors to be $f_M \approx 0.7$, $f_R \approx 2.0$ and $f_g \approx -3.3$, constant to about 10%. However, it is advisable to approach the construction of the calibrations separately for each region, since, as we will see in Sect. 4, the assumed -10 factor is not constant for all photometric regions.

The equations for $\log M$, $\log R$ and $\log g$ are obviously not independent, since there exists a linear relationship between them: $\log g = \text{cst.} + \log M - 2 \log R$. Thus, from Eq. (1) and the previous expression we obtain that $f_g = f_M - 2f_R$. Nevertheless, the three equations for $\log M$, $\log R$ and $\log g$ will be explicitly shown in the following sections basically to facilitate their application.

As commented in Paper I, the number of evolved stars within the sample is low, especially for the early region. Therefore, to provide an appropriate coverage of the different evolutionary phases from the ZAMS to the termination age (TAMS) of the main sequence, we have also used points in the form of synthetic stars from the evolutionary tracks by SSMM (adopting $Z=0.02$ for the metal content). The Strömgen-Crawford indices for these points were computed by using the theoretical predictions for T_{eff} and $\log g$ from the models and the interpolation of Napiwotzky et al. (1993, hereafter NSW) applied to the photometric grids of Moon & Dworetzky (1985, hereafter MD). Moreover, we considered the correction to the photometric surface gravity of the early region given by Eq. (2) of Paper I. As we will see in the next subsections, we thus obtained a uniform distribution of "stars" spread over a wide range of evolutionary stages with such a procedure. These synthetic stars were used first to check the expected agreement with the observational data from our sample as well as the potential relevance of chemical composition differences. After this, they were used to compute the f_q evolutionary coefficients.

3.1. ZAMS relations

To establish the unknown coefficients of Eq. (1), a relation between masses, radii, surface gravities and photometric indices (c_T and c_g) is needed. Even though we have adopted a ZAMS as reference relation, this is not strictly necessary. The validity of the formal expressions should remain when changing the reference line, i.e. we only need the f_q coefficients to be consistent with the relation adopted.

The best way to define a ZAMS relation in general is by using a sample of non-evolved eclipsing binary stars to trace a lower envelope, defining all needed parameters in a purely observational way and thus, completely model-independent. However, the number of eclipsing binary systems in the sample near the ZAMS is too low to attempt such a definition. In this situation, there are two different, although not completely indepen-

dent, ways to define the ZAMS. On one hand, stellar evolutionary models provide a “theoretical” ZAMS giving M , R and $\log g$ for different T_{eff} , which can be related to the photometric indices by means of the photometric grids. On the other hand, the “observational” ZAMS defined from colour-colour diagrams can be related to M , R and $\log g$ through the photometric grids and the evolutionary models. These latter calculations obviously cannot be performed when the observational ZAMS is below the theoretical one (i.e. if for a given effective temperature, the surface gravity of the observational ZAMS is larger than that of the theoretical value). To avoid this, we have adopted the first theoretical ZAMS definition using ZAMS of SSMM evolutionary models for solar metallicity (i.e. $Z = 0.02$). The ZAMS relations for the early, intermediate and late regions are listed in Tables 3, 4 and 5, respectively.

3.2. Early region

As stated in Paper I, stellar atmosphere models (Kurucz 1979, 1991) used to build photometric grids may not provide reliable surface gravity determinations for stars with $T_{\text{eff}} > 20000$ K. For stars with $11000 \text{ K} < T_{\text{eff}} < 20000 \text{ K}$, the correction proposed in Paper I yields an accuracy in the determination of surface gravity of 0.07 dex. Due to the expected uncertainties for stars hotter than 20000 K, we restricted our study to T_{eff} lower than this value.

Fig. 1 shows the relation between $\log q - \log q_{\text{ZAMS}}(c_o)$ and $\Delta\beta$ for both synthetic stars and 17 real stars. The agreement between the synthetic and the real stars is remarkable, even for the more evolved cases in the sample. The linearity of the relation is also clearly shown, and the use of the correction given in Paper I substantially improves both the linearity of the synthetic stars and their compatibility with the real ones.

The calibration obtained for each physical parameter has the following expression:

$$\begin{aligned} \log M &= \log M_{\text{ZAMS}}(c_o) + 1.77 \Delta\beta(c_o) \\ \log R &= \log R_{\text{ZAMS}}(c_o) + 4.88 \Delta\beta(c_o) \\ \log g &= \log g_{\text{ZAMS}}(c_o) - 7.99 \Delta\beta(c_o) \end{aligned} \quad (2)$$

These expressions are valid for main sequence stars with $11000 \text{ K} < T_{\text{eff}} < 20000 \text{ K}$. The mean residuals of the real stars in the sample are $\sigma_{\log M} = 0.027$ dex, $\sigma_{\log R} = 0.046$ dex and $\sigma_{\log g} = 0.08$ dex. Metallicity effects in this early region can be ignored.

3.3. Intermediate region

As shown in Fig. 2, the number of stars in the observational sample that belong to the intermediate region is very low. Nevertheless, we again find a good agreement between synthetic and real stars. Therefore, we were able to compute the calibrations for each of the physical parameters and obtain the following values:

$$\begin{aligned} \log M &= \log M_{\text{ZAMS}}(a_o) + 1.55 \Delta r(a_o) \\ \log R &= \log R_{\text{ZAMS}}(a_o) + 4.14 \Delta r(a_o) \\ \log g &= \log g_{\text{ZAMS}}(a_o) - 6.74 \Delta r(a_o) \end{aligned} \quad (3)$$

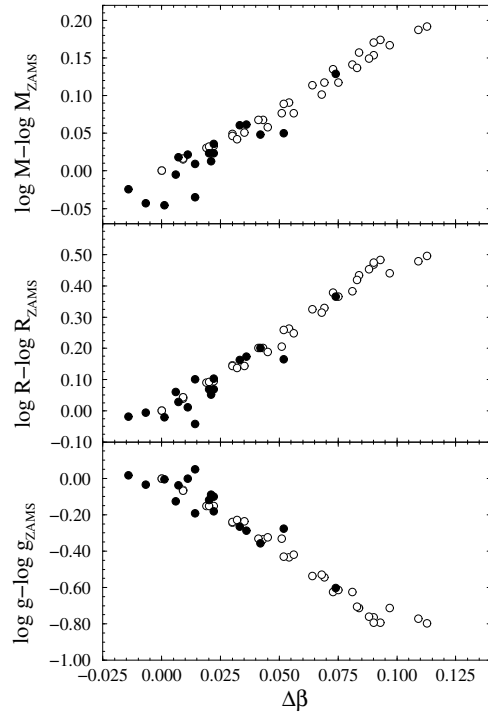


Fig. 1. Mass, radius and surface gravity calibrations as a function of an evolutionary term for the early region. Filled circles are real stars whereas open circles are synthetic stars

where $\Delta r = r - r_{\text{ZAMS}}(a_o)$. These calibrations are valid for main sequence stars with $8500 \text{ K} < T_{\text{eff}} < 11000 \text{ K}$. The mean residuals of the real stars in the sample are: $\sigma_{\log M} = 0.041$ dex, $\sigma_{\log R} = 0.057$ dex and $\sigma_{\log g} = 0.10$ dex.

The small number of stars with good photometric data and absolute dimensions in this region did not allow us to analyze corrections for the abundance effects, though their influence may not be negligible. For example, Andersen (1991) pointed out important metallicity effects for VV Pyx AB, and this system shows the largest residual in the $\log M$ plot in Fig. 2. However, the discrepancy is not observed in the $\log R$ or $\log g$ plots.

3.4. Late region

The late region can be divided into two subregions (splitting at $\beta = 2.72$, i.e. $T_{\text{eff}} = 7000 \text{ K}$), roughly A and F stars, with different trends, as shown in Paper I. First, we will focus on the hotter subregion including stars with $\beta > 2.72$ ($7000 \text{ K} < T_{\text{eff}} < 8500 \text{ K}$, A stars) and later in this section we will discuss the behaviour of stars with $\beta < 2.72$ ($6000 \text{ K} < T_{\text{eff}} < 7000 \text{ K}$, F stars).

As seen in Fig. 3, synthetic stars in the hot subregion show a well defined linear behaviour, but the real stars have a much larger dispersion, even though the general trend is similar. The reason for this different behaviour is changes in chemical composition. While all the synthetic stars have the same chemical composition ($Z = 0.02$), the stars in our observational sample present important variations.

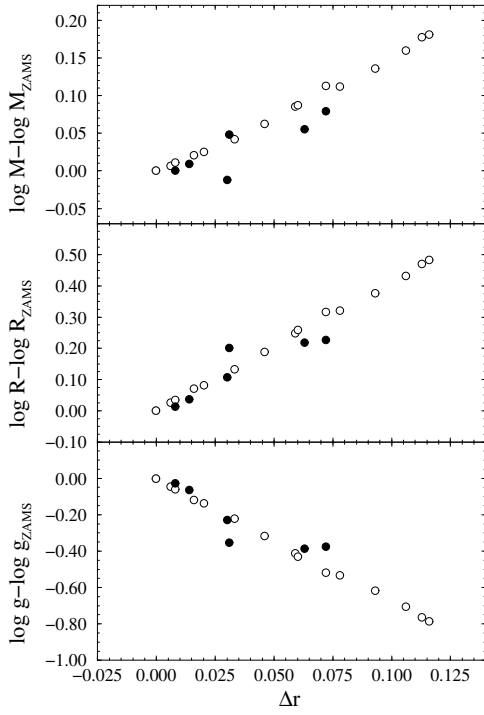


Fig. 2. Same as Fig. 1 for the intermediate region

A linear least squares fit of the synthetic stars for each of the physical parameters provides values of 0.64, 1.80 and -2.97 for the f_q coefficients. The derived mean residuals for the real stars are then: $\sigma_{\log M} = 0.039$ dex, $\sigma_{\log R} = 0.116$ dex and $\sigma_{\log g} = 0.19$ dex, which are roughly a factor of two larger than those of the early region. Since the cause of the dispersion is likely to be the presence of stars with different metallicities, we further analyzed the residuals as a function of a photometric index related to the metallicity. Fig. 4 shows a plot of the aforementioned residuals with respect to δm_o , and the correlation is obvious. Thus, an additional linear term with δm_o was considered in the calibrations to obtain:

$$\begin{aligned} \log M &= \log M_{\text{ZAMS}}(\beta) + 0.64 \delta c_o(\beta) - 1.11 (\delta m_o(\beta) + 0.005) \\ \log R &= \log R_{\text{ZAMS}}(\beta) + 1.80 \delta c_o(\beta) - 3.44 (\delta m_o(\beta) + 0.005) \\ \log g &= \log g_{\text{ZAMS}}(\beta) - 2.97 \delta c_o(\beta) + 5.77 (\delta m_o(\beta) + 0.005) \end{aligned} \quad (4)$$

which are applicable to stars in the main sequence belonging to the late region and with $T_{\text{eff}} > 7000$ K. The derived mean residuals are $\sigma_{\log M} = 0.021$ dex, $\sigma_{\log R} = 0.050$ dex and $\sigma_{\log g} = 0.08$ dex for the real stars in the data sample. These values are now very similar to those obtained for the early and intermediate regions. The zero point in δm_o takes into account that SSMM evolutionary models were built for solar metallicity ($Z = 0.02$) yielding $\delta m_o = -0.005$ for both the synthetic stars and the ZAMS (using Smalley's (1993) expression relating $[Fe/H]$ to δm_o).

Guthrie (1987) studied the influence of the metallicity effects on the evolutionary index δc_o , and defined a new $\delta c'_o = \delta c_o - 1.2 \delta m_o$, which only accounts for the evolution of the star. By using this definition, the previous equations can be reformulated to include the contribution of δm_o both in the ZAMS relation and in the δc_o index:

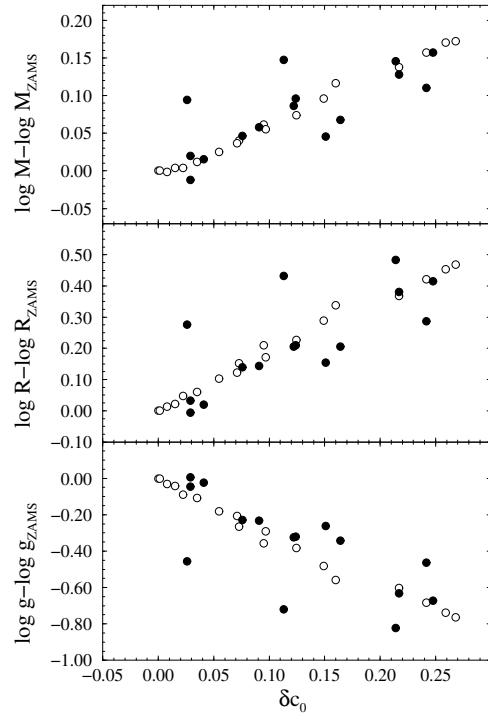


Fig. 3. Same as Fig. 1 for the late region ($\beta > 2.72$)

and considering new reference lines $\log q'_{\text{ZAMS}}$ that are dependent on δm_o :

$$\begin{aligned} \log M &= \log M'_{\text{ZAMS}} + 0.64 \delta c'_o \\ \log R &= \log R'_{\text{ZAMS}} + 1.80 \delta c'_o \\ \log g &= \log g'_{\text{ZAMS}} - 2.97 \delta c'_o \end{aligned} \quad (5)$$

$$\begin{aligned} \log M'_{\text{ZAMS}} &= \log M_{\text{ZAMS}} - 0.33 \delta m_o - 0.006 \\ \log R'_{\text{ZAMS}} &= \log R_{\text{ZAMS}} - 1.28 \delta m_o - 0.017 \\ \log g'_{\text{ZAMS}} &= \log g_{\text{ZAMS}} + 2.21 \delta m_o + 0.029 \end{aligned} \quad (6)$$

This new formulation in terms of $\delta c'_o$ and $\log q'_{\text{ZAMS}}$ allows us to plot Fig. 5, which is similar to Fig. 3, but takes metallicity effects into account. The initial dispersion has been greatly reduced by including a new term depending on δm_o , and the agreement between real and synthetic stars is quite good.

$\log q'_{\text{ZAMS}}$ are actually different ZAMS relations for different metallicities, showing how the physical parameters of the ZAMS change as a function of δm_o for a given β . These corrections to the ZAMS depending on the chemical composition were tested by using the evolutionary models computed by the Geneva group (SSMM, Schaerer et al. 1993a, 1993b, and Charbonnel et al. 1993) for several metallicities ranging from $Z = 0.001$ to $Z = 0.040$. We used Smalley's (1993) calibration relating the $[Fe/H]$ parameter (in our case computed through Z) to the δm_o index. For $7000 \text{ K} < T_{\text{eff}} < 8500 \text{ K}$ the stellar surface gravity of a ZAMS relation is nearly constant in T_{eff} but dependent on the metallicity (of the model). We performed

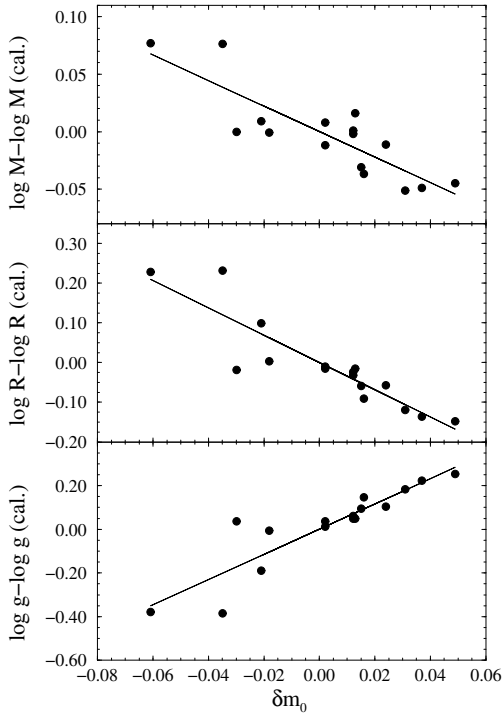


Fig. 4. Differences between the empirical $\log g$ and the determination using $f_M = 0.64$, $f_R = 1.80$ and $f_g = -2.97$ vs. δm_\odot for the late region ($\beta > 2.72$). The linear least squares fit to the stars is shown as a straight line

a linear least squares fit to the mean value of the surface gravity of each ZAMS as a function of δm_\odot , deriving a slope of 2.00 ± 0.13 , with a correlation coefficient of $\rho = 0.994$. This shows how the surface gravity of the stars on the ZAMS changes as a function of δm_\odot for a given T_{eff} . It is important to notice that in the definition of $\log q'_{\text{ZAMS}}$ the free parameter is β instead of T_{eff} . For a given metallicity, $T_{\text{eff}} \approx \text{const.}$ means $\beta \approx \text{const.}$, but in this case we consider different metallicities and this is no longer satisfied. In any case, since $\log g$ is nearly constant for a range of T_{eff} , the value of the previous slope can be directly compared with the value of 2.21 derived for the real stars. The verification of the $\log M'_{\text{ZAMS}}$ and $\log R'_{\text{ZAMS}}$ expressions is not possible, unless we know how the β index varies as a function of the metallicity, since the mass and the radius for the ZAMS are not just a function of the metallicity but also of the T_{eff} .

Finally, we will briefly deal with the coolest stars in this region, having $\beta < 2.72$, i.e. $6000 \text{ K} < T_{\text{eff}} < 7000 \text{ K}$. Fig. 6 shows no clear trend for the real stars and a relatively large dispersion of the synthetic stars with non-linear behaviour. When plotting the residuals of the real stars from a least squares fit to the synthetic ones, no clear correlation with the metallicity index δm_\odot was observed. The large uncertainties in the photometric surface gravity determination through model atmospheres, which are discussed in Paper I, may have a negative influence on the precision of the ZAMS relation, the synthetic stars, and, accordingly, on the attempted calibrations. The lack of linearity could also be due to the physics involved, which may not al-

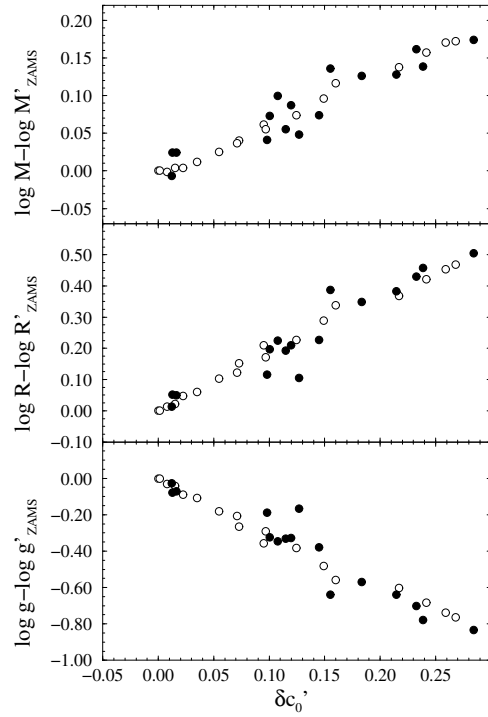


Fig. 5. Same as Fig. 1 for the late region ($\beta > 2.72$). Metallicity effects are included in the definition of $\log M'$, $\log R'$, $\log g'$ and $\delta c'_\odot$ (see text)

low us to establish simple linear relations. Thus, in the present situation it is not advisable to suggest any calibration for this subregion.

4. Discussion

As mentioned in Sect. 1, an accurate estimation of the mass, radius and surface gravity for single stars can be performed through stellar atmosphere and evolutionary models by means of Strömgren-Crawford photometric indices. Of course, an accurate determination can be obtained only in double-lined eclipsing binaries. Nevertheless, Table 1 shows that the calibrations presented in this paper, Eqs. (2), (3) and (4), reach a similar level of precision to that attained by direct interpolation in the models, with a much simpler procedure. This is in principle an unexpected result since, apparently, the enormous amount of information contained in the atmosphere models is not used at all. In fact, this information is present in the reference relation, which gives the physical parameters of a star for a well defined evolutionary status. The good accuracy of the calibrations is strongly related to the observed linearity of the relations, and it is useful that the physical parameters of different stars at the same effective temperature change in such a simple way as a function of the evolutionary status, at least within the main sequence.

However, we still cannot match the internal dispersion of the entry data although a carefully selected sample of detached eclipsing binaries was used. Some uncorrected abundance effects may have a negative influence on the accuracy. In the

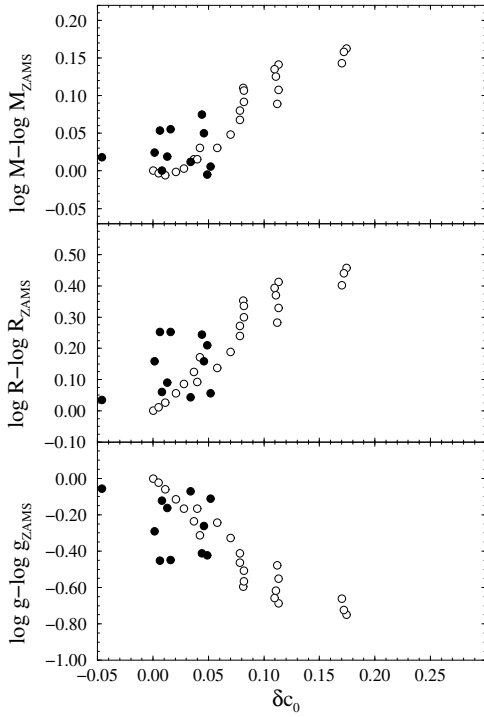


Fig. 6. Same as Fig. 1 for the late region ($\beta < 2.72$)

Table 1. Mean residuals in $\log M$, $\log R$ and $\log g$ of different calibrations with respect to the empirical determinations. The calibrations used are, on one hand, those including the interpolation in MD grids (applying the corrections given in Paper I) and in the evolutionary models by SSMM, and on the other hand, the calibrations presented in this work (Eqs. (2), (3) and (4))

Region	MD grids + SSMM models			This work		
	$\sigma_{\log M}$	$\sigma_{\log R}$	$\sigma_{\log g}$	$\sigma_{\log M}$	$\sigma_{\log R}$	$\sigma_{\log g}$
Early	0.024	0.039	0.07	0.027	0.046	0.08
Int.	0.031	0.055	0.09	0.041	0.057	0.10
Late [†]	0.018	0.053	0.10	0.021	0.050	0.08

[†] Only stars with $\beta > 2.72$

late region, three stars show a particularly large residual, in $\log M$, $\log R$ and $\log g$, two of which (AI Hya A, KW Hya A) have metallic spectra and the third (GZ CMa B) belongs to a system with a metallic-spectrum primary component. If these three stars are not taken into account, the mean residuals obtained from Eq. (4) are $\sigma_{\log M} = 0.017$ dex, $\sigma_{\log R} = 0.021$ dex and $\sigma_{\log g} = 0.03$ dex, a very significant improvement, which leads to precisions of 4-5% in both masses and radii. However, YZ Cas A, also quoted as an Am star, does not show a large residual. Abundance effects were also observed in the intermediate region (VV Pyx) but could not be corrected for due to the small number of stars in the sample. Another source of uncertainty is the precision of the photometric data. Photometry of eclipsing binaries is, in general, of lower quality than that of single stars. The reason for this is inherent to the calculation of the individual indices through the luminosity ratios which

Table 2. Evolutionary coefficients for the synthetic and real stars using the same expressions as those quoted in Eq. (1) but using ΔM_V as evolutionary term. ρ represents the correlation coefficient of the linear least squares fit. $k = \Delta M_V / \delta c_g$, using $\delta c_g = \delta c'_g$ for the late region. The values quoted by Andersen (1991) are $f_M \approx 0.7$, $f_R \approx 2.0$ and $f_g \approx -3.3$ using $k = -10$ in all photometric regions

Region	$\log q$	f_q	ρ	k		
Early	$\log M$	-0.0739 ± 0.0016	-0.975	-23.9	a	
		-0.0687	0.0066	-0.906	-25.8	b
	$\log R$	-0.2086	0.0016	-0.997	-23.4	a
		-0.2115	0.0120	-0.964	-23.1	b
	$\log g$	0.3433	0.0036	0.994	-23.3	a
		0.3547	0.0220	0.957	-22.6	b
Int.	$\log M$	-0.0743 ± 0.0010	-0.999	-20.9	a	
	$\log R$	-0.1985	0.0004	-1.000	-20.9	a
	$\log g$	0.3228	0.0016	1.000	-20.9	a
Late	$\log M$	-0.0758 ± 0.0021	-0.978	-8.7	a	
		-0.0724	0.0111	-0.830	-9.1	b
	$\log R$	-0.2045	0.0008	-1.000	-8.6	a
		-0.1879	0.0133	-0.956	-9.4	b
	$\log g$	0.3332	0.0028	0.998	-8.6	a
		0.3032	0.0276	0.930	-9.4	b

a: Simulations with evolutionary tracks; b: Stars in the sample

carries larger errors, especially for the least luminous star in the system. The overall result is thus that the suggested simple relations are remarkably linear, but may not be able to describe the physical parameters of a star with the accuracy of the entry data.

The values of the f_q coefficients computed using both real stars and synthetic stars are not exactly the same as those quoted by Andersen (1991). To explain this discrepancy we reformulated Eq. (1) using $\Delta M_V(c_T) = M_V - M_{VZAMS}(c_T)$ as the evolutionary term instead of δc_g . Similar calculations to those presented in Sect. 3 for both real and synthetic stars were performed. The absolute magnitudes for the real stars were taken from Andersen (1991), Nordström & Johansen (1994a, 1994b) and Clausen (1996), and for the synthetic stars they were computed from the luminosity quoted in the evolutionary models and the bolometric correction of Schmidt-Kaler (1982). The bolometric correction has negligible effect over the final result, as we computed differences of absolute magnitude nearly at the same effective temperature, and so, $\Delta M_V(c_T) \approx \Delta M_{bol}(c_T)$. The evolutionary coefficients (f_q) obtained are presented in Table 2 for the synthetic and real stars. No computation was performed in the intermediate region for the real stars because there were few of them. The agreement between the simulations with evolutionary models and the real stars is again very good. The evolutionary coefficients obtained are compatible with those quoted by Andersen (1991) if we assume a -10 factor when relating δc_g and ΔM_V . In Table 2 it is also shown that this factor is not constant for all regions. In the late region the coefficient is in better agreement with the -9 value found by Crawford (1979). For the intermediate region, the slopes are slightly larger in ab-

Table 3. ZAMS relation for the early region. T_{eff} , M , R and $\log g$ from SSMM and c_o and β from MD grids and NSW interpolation using the correction in $\log g$ proposed in Paper I

c_o	β	T_{eff} (K)	M/M_{\odot}	R/R_{\odot}	$\log g$ (cgs)
0.175	2.682	19980	6.460	3.078	4.272
0.200	2.687	19310	6.100	2.975	4.276
0.225	2.693	18670	5.760	2.876	4.281
0.250	2.699	18090	5.460	2.786	4.285
0.275	2.705	17580	5.200	2.707	4.289
0.300	2.710	17110	4.970	2.636	4.292
0.325	2.715	16650	4.760	2.574	4.294
0.350	2.721	16170	4.550	2.511	4.296
0.375	2.726	15760	4.370	2.455	4.298
0.400	2.732	15370	4.200	2.402	4.300
0.425	2.737	15010	4.050	2.354	4.301
0.450	2.742	14680	3.915	2.311	4.303
0.475	2.748	14360	3.790	2.271	4.304
0.500	2.753	14070	3.680	2.234	4.305
0.525	2.759	13780	3.570	2.198	4.306
0.550	2.764	13520	3.470	2.164	4.307
0.575	2.770	13280	3.380	2.133	4.308
0.600	2.776	13040	3.290	2.102	4.310
0.625	2.782	12820	3.210	2.074	4.311
0.650	2.789	12610	3.132	2.047	4.312
0.675	2.795	12410	3.060	2.021	4.312
0.700	2.802	12220	2.990	1.996	4.313
0.725	2.808	12030	2.928	1.974	4.313
0.750	2.815	11850	2.865	1.953	4.314
0.775	2.822	11670	2.808	1.932	4.314
0.800	2.829	11500	2.748	1.911	4.314
0.825	2.837	11320	2.690	1.891	4.314
0.847	2.843	11170	2.640	1.873	4.314
0.850	2.844	11140	2.632	1.870	4.314
0.875	2.852	10970	2.575	1.849	4.315

Table 4. ZAMS relation for the intermediate region. T_{eff} , M , R and $\log g$ from SSMM and a_o and r from MD grids and NSW interpolation

a_o	r	T_{eff} (K)	M/M_{\odot}	R/R_{\odot}	$\log g$ (cgs)
-0.070	0.016	10830	2.530	1.832	4.315
-0.060	0.015	10640	2.470	1.810	4.315
-0.050	0.013	10450	2.410	1.787	4.315
-0.040	0.012	10270	2.355	1.767	4.315
-0.030	0.009	10090	2.300	1.745	4.316
-0.020	0.007	9920	2.250	1.726	4.316
-0.010	0.006	9750	2.200	1.706	4.316
0.000	0.004	9590	2.150	1.687	4.316
0.010	0.003	9450	2.110	1.670	4.317
0.020	0.002	9340	2.065	1.652	4.317
0.030	0.001	9160	2.024	1.635	4.317
0.040	0.001	9000	1.980	1.618	4.317
0.050	0.001	8860	1.940	1.602	4.316
0.060	0.002	8710	1.900	1.587	4.315
0.070	0.003	8580	1.864	1.574	4.315

solute value than -17 , which was quoted by Strömgen (1966). The discrepancy in the coefficient for the early region is explained, as previously stated, by the qualitatively different construction of Crawford's (1978) absolute magnitude calibration. He used $\Delta M_V(\beta) = M_V - M_{V\text{ZAMS}}(\beta)$ and our definition is $\Delta M_V(c_o) = M_V - M_{V\text{ZAMS}}(c_o)$.

The full analysis and calculation of the coefficients in Eq. (1) was also performed using the ZAMS and the synthetic stars from the evolutionary models computed by Claret & Giménez (1992) and Bressan et al. (1993) at $Z = 0.02$. The linear trend of $\Delta \log g$ with respect to δc_g was again clearly present. The f_q coefficients slightly change since the reference line is different, but the final accuracies of the calibrations, estimated through the residuals of real stars were almost identical.

Table 5. ZAMS relation for the late region ($\beta > 2.72$) ($T_{\text{eff}} > 7000$ K). T_{eff} , M , R and $\log g$ from SSMM, β and c_o from MD grids and NSW interpolation and m_o (β) from Crawford (1979)

β	c_o	m_o	T_{eff} (K)	M/M_{\odot}	R/R_{\odot}	$\log g$ (cgs)
2.900	0.985	0.194	8560	1.860	1.572	4.314
2.890	0.956	0.197	8440	1.827	1.559	4.314
2.880	0.927	0.200	8350	1.802	1.549	4.313
2.870	0.897	0.203	8265	1.780	1.540	4.313
2.860	0.868	0.205	8190	1.760	1.532	4.313
2.850	0.841	0.207	8115	1.740	1.524	4.312
2.840	0.816	0.208	8040	1.720	1.516	4.312
2.830	0.794	0.207	7960	1.700	1.508	4.311
2.820	0.775	0.206	7875	1.680	1.501	4.311
2.810	0.760	0.205	7795	1.660	1.493	4.310
2.800	0.746	0.203	7710	1.640	1.486	4.308
2.790	0.730	0.200	7610	1.617	1.478	4.307
2.780	0.715	0.196	7530	1.598	1.470	4.306
2.770	0.696	0.192	7440	1.578	1.463	4.305
2.760	0.675	0.188	7360	1.558	1.456	4.304
2.750	0.652	0.185	7285	1.540	1.449	4.303
2.740	0.629	0.182	7205	1.522	1.442	4.302
2.730	0.605	0.179	7125	1.502	1.434	4.301
2.720	0.579	0.177	7050	1.477	1.410	4.309

Balona (1994) suggested mass and surface gravity calibrations computed through polynomial fits to the evolutionary models of Claret & Giménez (1992) and SSMM. The polynomial expression for the mass is a function of the effective temperature and the luminosity of the star, whereas the surface gravity is obtained through the c_o and β indices. By using these calibrations, we computed masses and surface gravities for the stars in our sample. To obtain the luminosities we used Strömgen-Crawford photometric indices, the absolute magnitude calibrations of Balona & Shobbrook (1984), Strömgen (1966) and Crawford (1979) for the early, intermediate and late regions, respectively, and the bolometric correction calibration of Balona (1994). The mean residual in $\log M$ was equivalent to that derived from the biparametric calibrations proposed in the present work, except for the late region where the residual is almost a factor of two larger, probably due to the abundance effects that were not taken into account by Balona (1994). The mean residuals in $\log g$ and, accordingly, in $\log R$ are much larger, but, as pointed out by the author, the surface gravity calibrations suggested in that work may not be reliable enough.

5. Conclusions

Using a sample of 53 stars belonging to 30 detached double-lined eclipsing binaries with accurate (≈ 1 -2%) determinations of masses and radii, we present photometric calibrations for the mass, radius and surface gravity of single stars in terms of Strömgen-Crawford photometric indices. The calibrations are based on those suggested by Andersen (1991) and have a similar formal expression to Crawford's (1975, 1978, 1979) absolute magnitude calibrations. Basically, a ZAMS reference relation and two photometric indices, one related to T_{eff} and another related to evolution, were used to build such calibrations.

We considered the separation of the stars in the sample into three different photometric regions and both a ZAMS relation and a calibration depending on suitable indices were considered for each region. Due to the lack of unevolved stars in the sam-

ple to define a purely observational ZAMS relation, we used that of SSMM evolutionary models, which was related to the photometric indices by means of the MD grids and NSW interpolation. Additionally, a simulation using SSMM evolutionary tracks was performed in order to consider a set of synthetic stars spread over a wide range of evolutionary stages within the main sequence, for a better definition of the linear calibrations attempted. The agreement between real and synthetic stars was excellent in all photometric regions. An additional linear term in δm_{\odot} was considered in the calibrations of the late region to account for abundance effects. Although a similar treatment may also be necessary for the intermediate region, the lack of real stars in this region prevented an equivalent correction.

Thus, Eqs. (2), (3) and (4), together with Tables 3, 4 and 5 constitute the biparametric calibrations proposed in this work, applicable to main sequence stars with $7000 \text{ K} < T_{\text{eff}} < 20000 \text{ K}$. For both cooler and hotter stars, a suitable definition of the ZAMS relation and, accordingly, of the calibrations was not possible, as quoted in Paper I, due to the inaccuracies in the model atmospheres used to relate the photometric indices to T_{eff} and $\log g$. The mean residuals obtained for the real stars are very similar to those given by a more complex algorithm using MD grids and SSMM stellar evolutionary models, and better than those from single-parameter calibrations by a factor of about three.

Acknowledgements. This work was supported by the Spanish CICYT under contract ESP95-0180. I.R. acknowledges the grant of the *Beques predoctorals per a la formació d'investigadors* by the CIRIT (Generalitat de Catalunya)(ref. FI-PG/95-1.111).

References

- Allen, C.W., 1973, in: *Astrophysical Quantities*, 3rd. ed. Athlone, London, p. 209
- Andersen, J., 1991, *A&AR* 3, 91
- Asiain, R., Torra, J., Figueras, F., 1997, *A&A* (in press)
- Balona, L.A., 1984, *MNRAS* 211, 973
- Balona, L.A., 1994, *MNRAS* 268, 119
- Balona, L.A., Shobbrook, R.R., 1984, *MNRAS* 211, 375
- Becker, S.A., 1981, *ApJS* 45, 475
- Bressan, A., Fagotto, F., Bertelli, G., Chiosi, C., 1993, *A&AS* 100, 647
- Charbonnel, C., Meynet, G., Maeder, A., Schaller, G., Schaerer, D., 1993, *A&AS* 101, 415
- Claret, A., Giménez, A., 1992, *A&AS* 96, 255
- Clausen, J.V., 1996, *A&A* 308, 151
- Crawford, D.L., 1975, *AJ* 80, 955
- Crawford, D.L., 1978, *AJ* 83, 48
- Crawford, D.L., 1979, *AJ* 84, 1858
- Figueras, F., Torra, J., Jordi, C., 1991, *A&AS* 87, 319
- Guthrie, B.N.G., 1987, *MNRAS* 226, 361
- Habets, G.M.H.J., Heintze, J.R.W., 1981, *A&AS* 193
- Jordi, C., Ribas, I., Torra, J., Giménez, A., 1997, *A&A* (Paper I) (in press)
- Kurucz, R.L., 1979, *ApJS* 40, 1
- Kurucz, R.L., 1991, in: *Precision Photometry: Astrophysics of the Galaxy*, eds. A.G. Davis Philip, A.R. Upgren and K.A. Janes, L. Davis Press, Schenectady, p.27
- Maeder, A., 1981, *A&A* 102, 401
- Moon, T.T., Dworetzky, M.M., 1985, *MNRAS* 217, 305 (MD)
- Napiwotzky, R., Schönberner, D., Wenske, V., 1993, *A&A* 268, 653 (NSW)
- Nordström, B., 1989, *ApJ* 341, 934
- Nordström, B., Johansen, K.T., 1994a, *A&A* 282, 787
- Nordström, B., Johansen, K.T., 1994b, *A&A* 291, 777
- Schaerer, D., Meynet, G., Maeder, A., Schaller, G., 1993a, *A&AS* 98, 523
- Schaerer, D., Charbonnel, C., Meynet, G., Maeder, A., Schaller, G., 1993b, *A&AS* 102, 339
- Schaller, G., Schaerer, D., Meynet, G., Maeder, A., 1992, *A&AS* 96, 269 (SSMM)
- Schmidt-Kaler, T., 1982, in *Landolt-Börnstein*, eds. K. Schaifers and H.H. Voigt, Vol. II, Subvol. B, p. 30
- Smalley, B., 1993, *A&A* 274, 391
- Straizys, V., Kuriliene, G., 1981, *Ap&SS* 80, 353
- Strömgren, B., 1966, *ARA&A* 4, 433
- Van Hamme W., Wilson, R.E., 1986, *ApJ* 307, 151